

Power transmission analysis of coupled rectangular plates with elastically restrained coupling edge including in-plane vibration

CHEN Yuehua , JIN Guoyong, DU Jingtao and LIU Zhigang

College of Power and Energy Engineering, Harbin Engineering University, Harbin 150001, China

PACS: 43.40.Dx

ABSTRACT

A theoretical study on the power transmission characteristics of a U-shaped configuration consisted of three rectangular plates is presented. Four groups of springs, to simulate the transverse shearing forces, bending moments, in-plane longitudinal forces and in-plane shearing forces separately, are distributed consistently along each edge of the model. With general boundary condition of both flexural and in-plane vibrations taken into account by setting the stiffness of these springs, the double Fourier series solution to the dynamic response of the structure is obtained by employing the Raleigh-Ritz method. For model validation, the natural frequency and velocity response of the model are checked against existing literature results and the ANSYS data and good agreement is achieved. The influence of several relevant parameters on power transmission of the coupled structure is then systematically studied, including boundary conditions, coupling conditions, and locations of the external force.

1. INTRODUCTION

Power flow method, as an effective analytical technique on the dynamic response and energy distribution of structures, has been extensively investigated in recent years. Numerous studies, employing various methods, on the vibrational energy transmission analysis of rod, beam, plate and other complicate structures have been conducted in the basic understanding of these configurations [1-19]. Farag and Pan [9] present an analytical solution of two coupled rectangular plates connected at an arbitrary angle, basing on the receptance method. This coupling model, considering both flexural and in-plane vibration, is under simply supported boundary condition and excited by external point force and moment. In their previous work, the power flow of two in-plane coupled beam structures is also investigated [10]. Kessissoglou [13] examined the contribution of various wave types on the power flow of an L-shaped plate by using the combination of the modal method and the travelling wave method. The power analysis of an indeterminate beam system is investigated by Wang et al [16] adopting the substructure approach. This method is subsequently applied to investigate the power flow characteristics of an L-shaped plate, aiming to make clear how the power is distributed spatially within and across the plate [17]. The finite element method [15], energy method [4, 18, and 19], mobility power flow approach [11, 12], dynamic stiffness technique [14] and other means are employed to deal with various problems with the power flow technique.

It is widely accepted that the accuracy solution existed only for the plates simply supported along at least one pair of opposite edges. Li [20, 21] proposed an improved Fourier method to calculate the exact transverse solution of an elastically restrained rectangular plate. In the displacement receptance

expression, the auxiliary terms are added to overcome the potential discontinuity overall the whole plate area. The general boundary condition is simulated by changing the stiffness of the boundary springs, which is adopted in present paper. Subsequently, dynamic model of two coupled rectangular plates and the in-plane vibration of the rectangular plate with general boundary conditions is analysed by Du [22, 23] using this method. In the present article, an analytical model has been developed to investigate the dynamic response and power transmission of a U-shaped structure with elastically restrained boundary condition and coupling condition. Based on the thin plate theory, the double Fourier series solution to the dynamic response of a three coupled plate model is obtained by employing the Raleigh-Ritz method. The validation of the model is checked against the existing literature data. The parameters related to the power transmission are separately investigated, including the boundary conditions, coupling conditions, and locations of the external force.

2. THE MODEL OF THREE COUPLED PLATES

This model of three rectangular plates coupled in a U-shaped configuration with general boundary condition is developed using the Fourier series and Rayleigh-Ritz method, as shown in Fig. 1. Four sets of springs are distributed consistently along each edge to separately simulate the transverse and in-plane vibration including the bending moments, transverse shearing forces, in-plane longitudinal and shearing forces marked as, take the edge $x_1=a_1$ for example, K_{bx11} , k_{bx11} , $knx11$, $kpx11$, respectively. Another four sets of congener springs are arranged at the two coupling edges to describe the mutual internal effects of two plates and Fig.1 shows the coupling springs at the edge $x_1=0$. Considering the continuity of the displacement and its derivatives over the entire plate's area, the

admissible functions of the transverse and in-plane displacements are

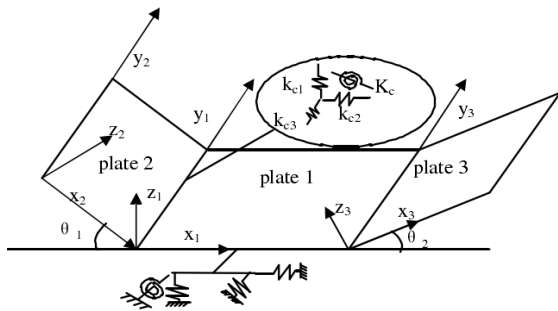


Figure.1 Schematic of a U-shaped model with general boundary condition and coupling condition

expressed as the sum of double Fourier series expansions and several auxiliary terms. The transverse admissible function is [21]

$$\begin{aligned}
 W(x,y) = & \sum_{m=0}^{\infty} \sum_{n=0}^{\infty} A_{mn} \cos \lambda_{am} x \cos \lambda_{bn} y + \zeta_{1b}(y) \sum_{m=0}^{\infty} a_m \cos \lambda_{am} x + \zeta_{2b}(y) \sum_{m=0}^{\infty} b_m \cos \lambda_{am} x \\
 & + \zeta_{3b}(y) \sum_{m=0}^{\infty} c_m \cos \lambda_{am} x + \zeta_{4b}(y) \sum_{m=0}^{\infty} d_m \cos \lambda_{am} x + \zeta_{1a}(x) \sum_{n=0}^{\infty} e_n \cos \lambda_{bn} y \\
 & + \zeta_{2a}(x) \sum_{n=0}^{\infty} f_n \cos \lambda_{bn} y + \zeta_{3a}(x) \sum_{n=0}^{\infty} g_n \cos \lambda_{bn} y + \zeta_{4a}(x) \sum_{n=0}^{\infty} h_n \cos \lambda_{bn} y
 \end{aligned} \tag{1}$$

And the in-plane admissible functions are [22]

$$u(x,y) = \sum_{m=0}^{\infty} \sum_{n=0}^{\infty} B_{mn} \cos \lambda_{am} x \cos \lambda_{bn} y \tag{2}$$

$$\begin{aligned}
 & + \zeta_{1b}(y) \sum_{m=0}^{\infty} a_{1m} \cos \lambda_{am} x + \zeta_{2b}(y) \sum_{m=0}^{\infty} b_{1m} \cos \lambda_{am} x \\
 & + \zeta_{1a}(x) \sum_{n=0}^{\infty} c_{1n} \cos \lambda_{bn} y + \zeta_{2a}(x) \sum_{n=0}^{\infty} d_{1n} \cos \lambda_{bn} y
 \end{aligned}$$

$$v(x,y) = \sum_{m=0}^{\infty} \sum_{n=0}^{\infty} C_{mn} \cos \lambda_{am} x \cos \lambda_{bn} y \tag{3}$$

$$\begin{aligned}
 & + \zeta_{1b}(y) \sum_{m=0}^{\infty} e_{1m} \cos \lambda_{am} x + \zeta_{2b}(y) \sum_{m=0}^{\infty} f_{1m} \cos \lambda_{am} x \\
 & + \zeta_{1a}(x) \sum_{n=0}^{\infty} g_{1n} \cos \lambda_{bn} y + \zeta_{2a}(x) \sum_{n=0}^{\infty} h_{1n} \cos \lambda_{bn} y
 \end{aligned}$$

where $\lambda_{am} = m\pi / a$, $\lambda_{bn} = n\pi / b$.

Based on the assumption of the standard theory of thin plates, the potential energy and kinetic energy of the model, marked as V&T separately, can be written as

$$\begin{aligned}
 V = & V_{1bending} + V_{1in-plane} + V_{2bending} + V_{2in-plane} \\
 & + V_{3bending} + V_{3in-plane} + V_{coupling}
 \end{aligned} \tag{4}$$

$$T = T_{1bending} + T_{1in-plane} + T_{2bending} + T_{2in-plane} + T_{3bending} + T_{3in-plane} \tag{5}$$

Then the Lagrange function can be obtained as

$$L = V - T \tag{6}$$

$V_{coupling}$ means the elasticity energy stored in the coupling springs. Make a differential calculate on the Lagrange function, these equations can be written in a matrix form as

$$(\mathbf{K} - \rho h \omega^2 \mathbf{M}) \mathbf{E} = 0 \tag{7}$$

Where, \mathbf{K} and \mathbf{M} is stiffness and mass matrix, \mathbf{E} is the unknown expansion coefficients matrix expressed as $\mathbf{E} = [\mathbf{A1} \ \mathbf{B1} \ \mathbf{C1} \ \mathbf{A2} \ \mathbf{B2} \ \mathbf{C2} \ \mathbf{A3} \ \mathbf{B3} \ \mathbf{C3}]^T$. By resolving the standard

matrix characteristic equation, natural frequencies and mode shapes can be easily obtained. In addition, when the model is excited by external force or/and moment, the eigenpairs can also be determined by simply adding a load vector to the right side of Eq. (7).

The time-averaged structural intensity of a thin plate in the x direction can be expressed as [16]:

$$P_x(\omega) = \int_0^b -\frac{1}{2} \text{Re} [Q_x(w)^* - M_x \left(\frac{\partial w}{\partial x} \right)^* - M_y \left(\frac{\partial w}{\partial y} \right)^* + (u)^* N_x + (v)^* N_y] dy \tag{8}$$

where the asterisk (*) means the complex conjugate.

3. NUMERICAL RESULTS AND DISCUSSION

With the theory described in previous section, several calculations are carried out firstly to quantify the accuracy of the model. Numerical analyses are subsequently performed to explore the effect of relevant parameters on the power transmission. The material properties and structural dimensions of the configuration are taken as follows. The three substructures are identically made of aluminium with $\rho = 2710 \text{ kg/m}^3$, Young's modulus $E = 72 \text{ GPa}$, Poisson ratio $\mu = 0.3$ damping $\eta = 0.01$, thickness $h = 0.00635 \text{ m}$ and coupled along the y-direction.

A. Model validation

As a validation, the natural frequency solutions are compared with the existing literature data [20, 21] and the ANSYS results, as shown in figures 2, 3 and tables 1, 2. Firstly, the flexural vibration of a square panel under different boundary condition is investigated by setting the coupling angles to 0 deg. The length of each plate is 1/3m, and the width is 1.0m. Then the model with an infinite coupling stiffness (1e10 N/m) turns to be a single square plate. Table 1 shows the first sixth natural frequency of a flat plate under CCCC and SSSS boundary condition respectively. The 'one plate' term in table 1 stands for the dimensional and dimensionless results for the single plate adopting the same material parameters as the three-coupled plate model. A good agreement is achieved. Figure 2 exhibits the fifth and sixth mode shape for a simply supported square plate, and the first and fourth mode for a C-F-F-F one. These four representative mode shapes are selected to prove the validation of the model in detail.

Table 1 Natural frequencies of a flat square plate

Mode No.	CCCC			
	Current[Hz]	One plate		Ref[21]
		Hz	dimensionless	
1	56.726	56.725	35.984	35.985
2	115.69	115.69	73.390	73.393
3	115.69	115.69	73.390	73.393
4	170.58	170.58	108.21	108.21
5	207.43	207.40	131.57	131.58
6	208.39	208.39	132.19	132.20

Mode No.	SSSS			
	Current[Hz]	One plate		Ref[20]
		Hz	dimensionless	
1	31.23	31.30	19.85	19.74
2	77.93	78.05	49.51	49.35
3	77.97	78.05	49.51	49.35
4	124.83	125.05	79.33	78.96
5	155.79	155.58	98.69	98.70
6	155.99	156.27	99.13	98.70

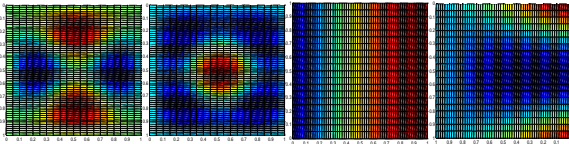


Figure.2 The fifth and sixth mode shape for a SSSS square plate and the first and fourth mode shape for the CFFF square plate

Next, a U-shaped plate model is resolved under a simply supported condition for the transverse vibration and a clamped condition for the in-plane vibration by setting the stiffness of all relevant springs to $1e10N/m$. (This boundary condition will be abbreviated as SS-CS in the following section.) The free junctions are also rigidly coupled. The eigen frequency results are given in Table 2 and the mode shapes are plotted in Fig.3. As a comparison, the ANSYS results derived from a model consisting of 100 linear rectangular elements along each edge, as expressed in table, are also listed. The responding parameters adopted in this and subsequent models are as follow: $a_1=a_2=a_3=0.5$ m, $b_1=b_2=b_3=1.5$ m and both the coupling angles are 90 degree. In table 2, current solutions for the U-shaped configurations are calculated and compared with the ANSYS results, when the series is truncated to 7 and 9. A visual comparison of mode shapes is shown in Fig.3. The results of these examples convincingly demonstrate that the present analytical model is reliable.

Table 2 First nine natural frequencies for a U-shaped plate

Mode No.	Current solution		ANSYS 100*100	difference %
	M=M=7	M=M=9		
1	69.531	69.359	69.117	0.35
2	85.513	85.629	85.447	0.21
3	90.871	90.448	89.848	0.67
4	104.77	104.48	103.99	0.47
5	121.20	121.14	121.04	0.08
6	126.78	125.67	124.40	1.02
7	136.52	136.37	136.10	0.20
8	138.08	137.17	136.13	0.76
9	164.73	164.29	163.77	0.32

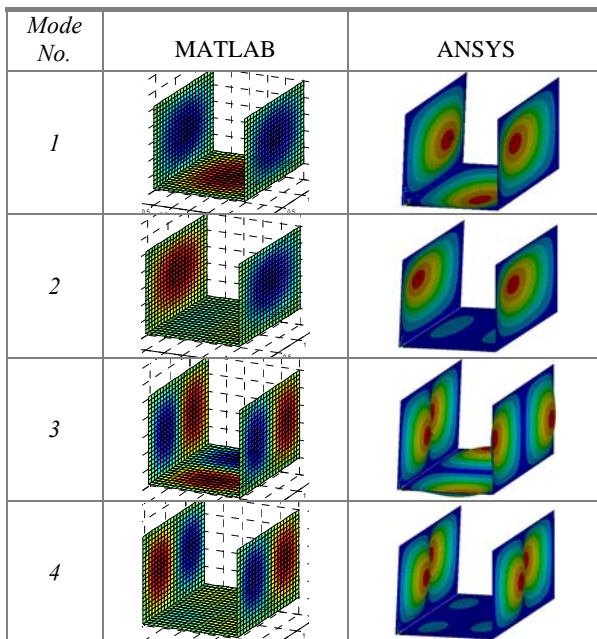


Figure.3 First four mode shapes of a U-shaped plate

A compared result of the U-shaped structure, as previously mentioned, is plotted to explore the effect of truncated series on the convergence in the range of 1000Hz. The calculated

frequencies in Fig.4, which are determined by truncating the series to 11, show an excellent agreement with the solution derived from ANSYS when the model is divided into 100 linear elements along each edge. Thus, in the following numerical calculations, the expansion series will be truncated to 11 and the structural properties will be kept the same as mentioned above.

Figure 5 compares the velocity response of the present method (purple line) with that of the FEM technique (blue line), both based on the SS-CS U-shaped model with an external harmonic excitation force imposed at the centre of plate 3 in the normal direction. The results of Fig. 5 (a) and (b) show the velocity response of the centre point of plate 2 & 3 separately and exhibit analogous trend, respectively. As the amplitude of the external force is 1N, these two figures also stand for the point mobility and the transfer mobility.

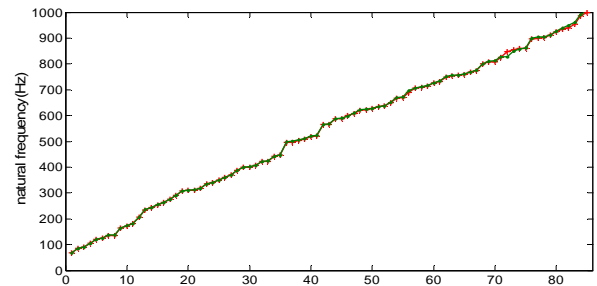
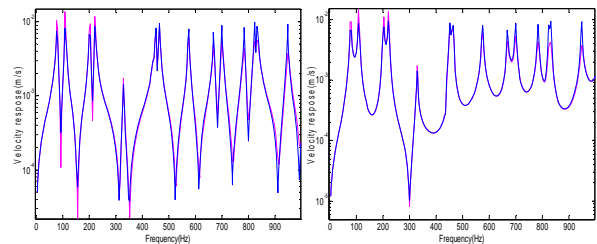


Figure 4 Comparison of natural frequencies of a U-shaped plate: + Results from ANSYS x Current results



(a) Point mobility (b) Transfer mobility

Figure 5 Velocity responses of the SS-CS U-shaped plate under normal excitation at the centre of plate 3: — velocity of present method — velocity of FEM method

B. Effects of boundary condition on power Transmission

The influence of boundary conditions on the power transmission of a U-shaped configuration is investigated in this section. In the model, the two coupling edges are rigidly connected and a normal excitation is loaded at the centre of plate 3. The curves of Fig.6, 7 and 8 separately present for SS-CS boundary condition, elastically restrained condition and free boundary condition, by changing the stiffness of responding springs from $1e10N/m$ to $1e5N/m$ or $1e-1N/m$. Fig.9 exhibits the first four time-averaged structural intensity vectors in three plates when the model is under a free boundary condition and loaded with a point excitation at the centre of plate 3.

As expected and consistent with the theory, it can be observed that, as the boundary restraint is decreased, the total resonant peaks increase (from 27 to 34 and 38) and the first natural frequency shifts to a lower frequency (from 70Hz to 15Hz and 12 Hz). Note that the total transferred power in plate 2 is holistically lower than that in plate 1 and the input power in plate 3. This is attributed to the fact that the power is transmitted in an actinomorphic way (Fig.9), and partly damped as the existing of damping. Another reason for the reduced power might be that power regurgitation occurs at the junction as show in Fig.9. In this figure, as the motion of the

edges, the trend of power flowed to the edges can be obviously observed.

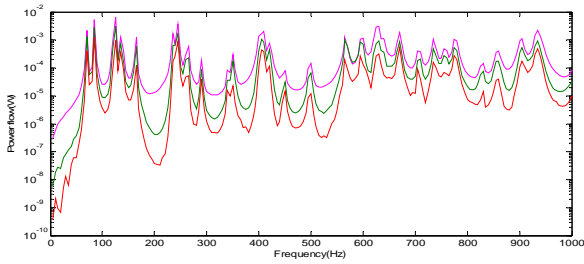


Figure 6 Power flow of a rigidly coupled U-shaped structure under SS-CS boundary condition: — Total input power — Total transferred power in plate 1 — Total transferred power in plate 2

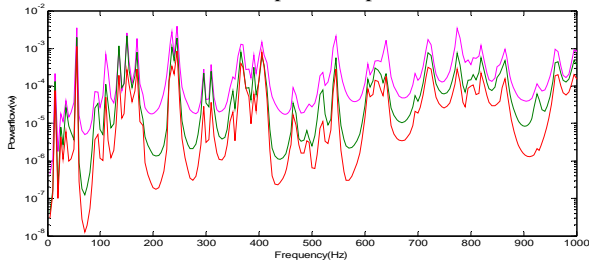


Figure 7 Power flow of a rigidly coupled U-shaped structure under elastically restrained boundary condition: — Total input power — Total transferred power in plate 1 — Total transferred power in plate 2

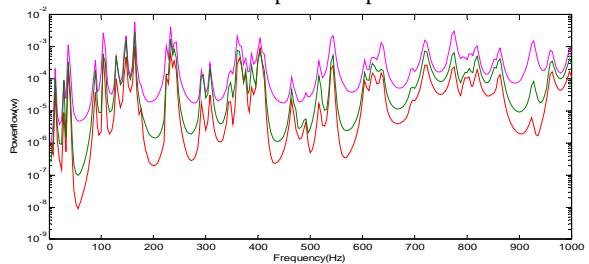
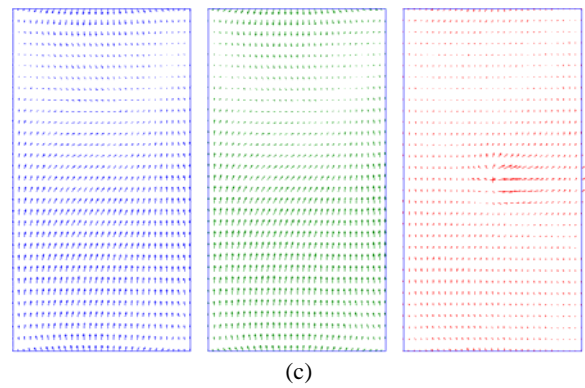
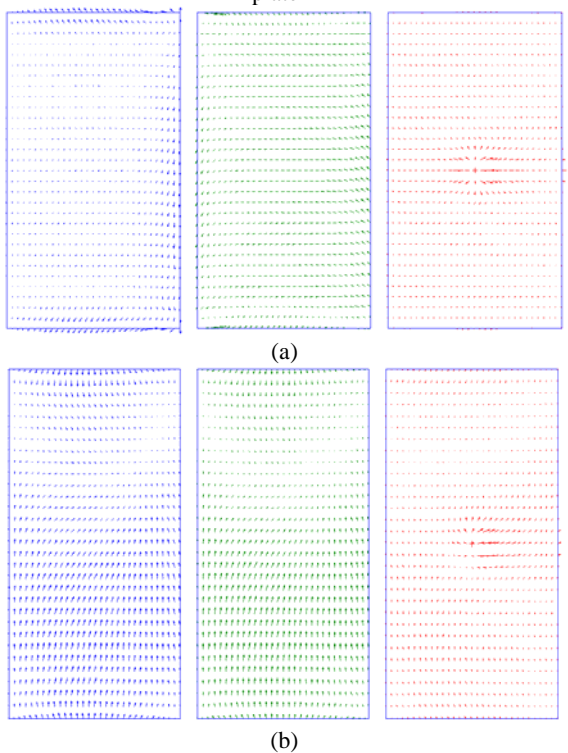
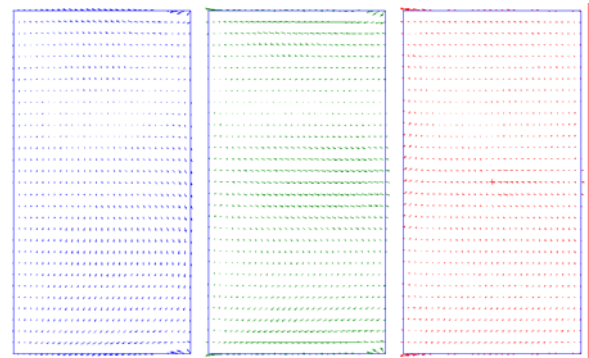


Figure 8 Power flow of a rigidly coupled U-shaped structure with a free boundary restraint: — Total input power — Total transferred power in plate 1 — Total transferred power in plate 2



(c)

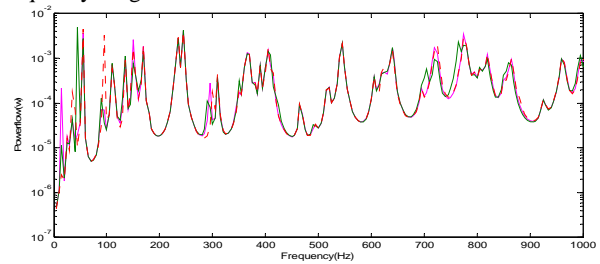


(d)

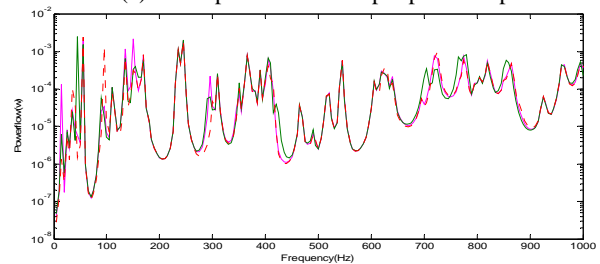
Figure 9 Time-averaged structural intensity vector in three plate, “+” indicates the excitation location excited at (a) the first (b) the second (c) the third (d) the fourth resonant frequency

C. Effects of coupling angles on power transmission

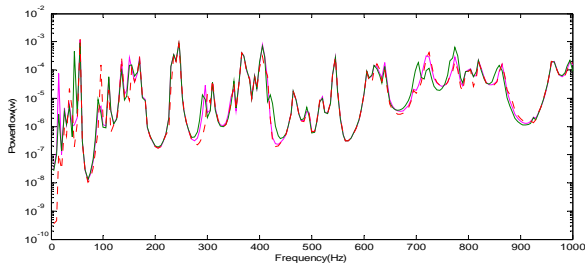
In order to explore the rules of coupling angles on power transmission, the power versus frequency curves are presented in Fig.10. The model adopted here is the one with elastically restraint boundary condition. The input power in plate 3, power transmitted in plate 1 and power transferred in plate 2 are separately compared in Fig.10 a, b & c when the coupling angle θ_1 is selected as 60° , 90° and 120° (whereas θ_2 remains be kept as 90°). It is of interesting to note that one more resonant frequency is excited in the 60° - 90° coupling model while in the other two models, the power at some peaks is enhanced. Generally speaking, the coupling angle plays a slight role in power transmission except several resonant peaks at low frequency range.



(a) Comparison of the input power in plate



(b) Comparison of the transferred power in plate 1



(c) Comparison of the transferred power in plate 2
Figure 10 effects of the coupling angle on power transmission: — 60°-90° model — 90°-90° model
 120°-90° model

D. Effects of the excitation location on the power transmission

Numerical studies are formed to quantify the influence of the excitation location on the power properties of a SS-CS U-shaped configuration with two elastically coupled edges. The external point force is imposed at the centre of plate 1. The curves of power versus frequency are plotted in Fig.11 and the first four time-averaged structural intensity vectors in three plates are shown in Fig.12. As the bilateral symmetry of the model, the curves of the power transferred to plate 2 and plate 3 are superposed, as shown in Fig.11, and the structural intensity vectors are also distributed symmetrical (Fig.12). Further more, it is worthwhile to note that the transferred power is largely deduced than the input power, owing to the main fact that both the two coupling edges are elastically connected and less energy is transmitted across the junctions.

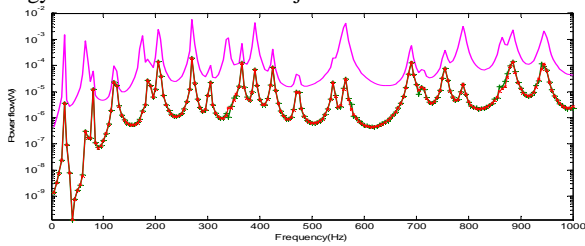
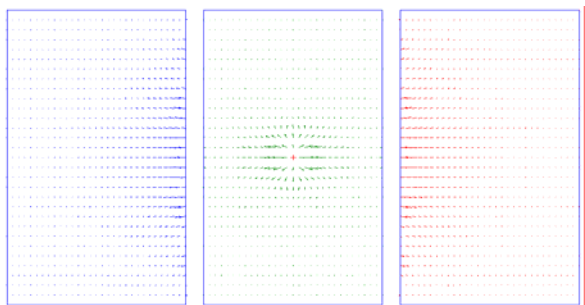
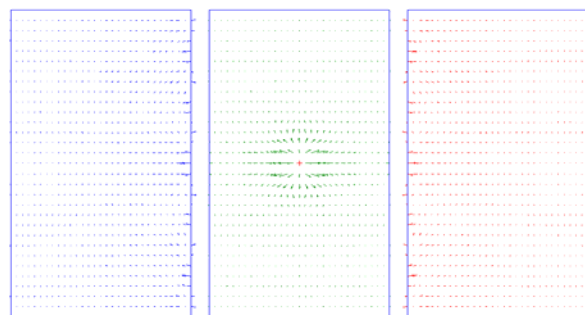


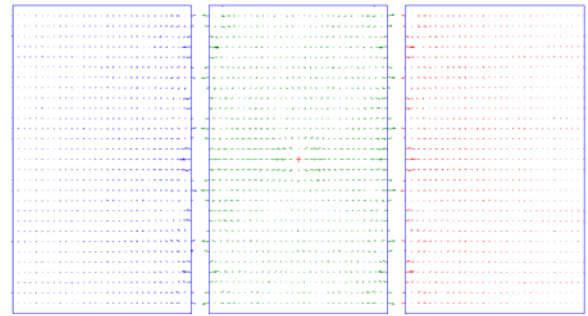
Figure.11 Power transmission of an elastically coupled U-shaped configuration excited at the centre of plate 1 — input power in plate 1 — power transferred in plate 2 — power transferred in plate 3



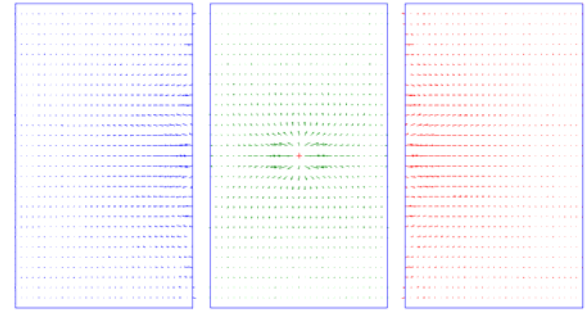
(a)



(b)



(c)



(d)

Figure.12 Structural intensity of an elastically coupled U-shaped configuration excited at the centre of plate 1: (a) first frequency (b) second frequency (c) third frequency (d) fourth frequency

Another U-shaped model with rigidly coupled edges under the SS-CS boundary condition is calculated when the external force is loaded at (0.15m, 0.75m) in plate 1. The total input power in plate 1 (purple line), the power transferred across the centre of plates 1 (green line) and the power transferred to plate 3 (red line) are presented in Fig.13. As mentioned above, the deduced power in plate 1 between the purple line and green line is caused, on one hand, by structural damping, on the other hand, by the power transferred in other directions. However, comparing the power transferred across the central line of plate 1 and plate 3, the margin is not only caused by the damping and the junction loss but also by the power circumfluence from plate 3 to plate 1, as shown in Fig. 14.

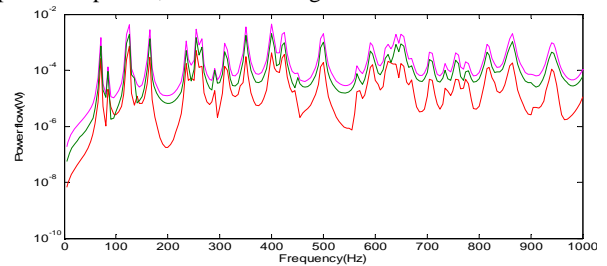
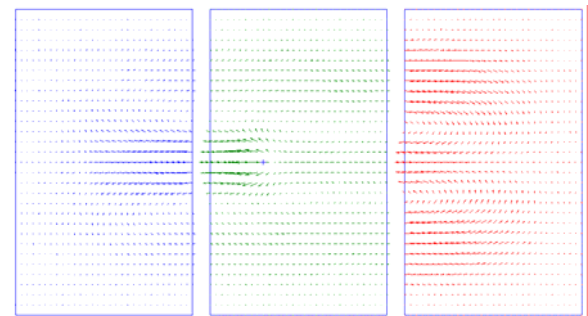


Figure.13 Power flow of a U-shaped plate with the excitation located at (0.15, 0.75) in plate 1: — Input power in plate 1 — power transmitted in plate 1 — power transmitted in plate 2



(a)

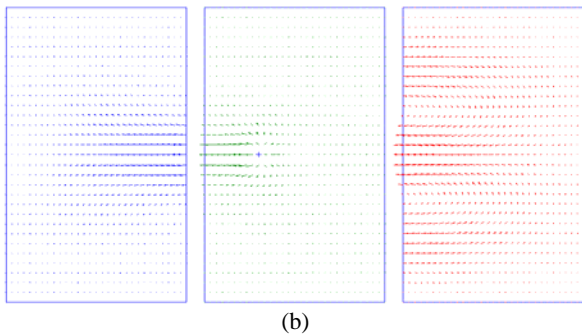


Figure.14 Structural intensity of a U-shaped plate with the excitation located at (0.15, 0.75) in plate 1: excited with the (a) second resonant frequency (b) third resonant frequency

E. Effects of the stiffness of the coupling springs on power transmission

To quantify the influence on the power transmission caused by the coupling stiffness, the power flow curves are calculated for the SS-CS U-shaped model with selected coupling condition: rigidly coupled condition (1e10N/m, Fig.6), elastically coupled condition (1e5N/m, Fig.15) and feebly coupled condition (1e0N/m, Fig.16). The external point force is loaded at the centre of plate 3. It can be observed that the first resonant peak shifts to a lower frequency as the coupling stiffness is decreased. As shown in Fig.16, the stiffness of the coupling springs is so small that very little energy is transmitted to plate 1 and much less power is transferred to plate 2. Theoretically, the power in plate 1 and plate 2 will equal to zero when the plates are unattached with each other.

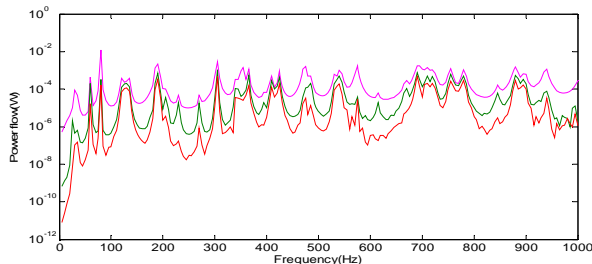


Figure.15 Power flow of an elastically connected U-shaped plate with the excitation located at the centre of plate 3 — input power in plate3 — transferred power in plate1 — transferred power in plate2

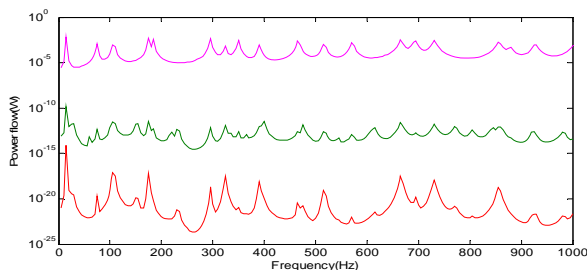


Figure.16 Power flow of a feebly connected U-shaped plate with the excitation located at the centre of plate 3 — input power in plate3 — transferred power in plate1 — transferred power in plate2

4 CONCLUSIONS

An analytical model has been developed to investigate the dynamic response and power transmission of a U-shaped structure with elastically restrained boundary condition and coupling condition. The double Fourier series solution to the dynamic response of the structure is obtained by employing the Raleigh-Ritz method. The validation of the model is checked with the existing literature results and the FEM method data by

several numerical cases, with excellent agreement achieved. The truncated number of the Fourier solution is determined by checking the convergence with the ANSYS data. In the consequent part of the article, the influence of several relevant parameters on power transmission of the coupled structure is studied, including boundary conditions, coupling conditions, and locations of the external force.

It is found that the power transmission of the structure can be significantly affected by altering the boundary condition without changing other parameters of the model. The decrease in stiffness of the boundary restraints considerably excites more resonant peaks and makes the first resonant peak shift to lower frequency. Conversely, the influence of the coupling angle on power flow is slight over the whole range except certain resonant points. It should be emphasized that the location of the excitation will remarkably influence the power transmission. Once the excitation is imposed on the central symmetry point of the model, the power transmitted will show a symmetrical distribution. When the location deviates from the central symmetry point, the power circumfluence occurs. Partly due to the power circumfluence, the power transmits across the junction with certain energy loss. Analogous to the effect of boundary restraint, as the decrease in coupling stiffness, the first resonant peak shifts to lower frequency. Theoretically, the transferred power in plate 1 and plate 2 will be zero when the plates do not interact with each other.

ACKNOWLEDGMENT

The authors acknowledge the support of this work by the National Natural Science Foundation of China (No.10802024), Research Fund for the Doctoral Program of Higher Education of China (No.200802171009), Natural Science Foundation of Heilongjiang Province (No.E200944) and Innovative Talents Fund of Harbin (No.2009RFQXG211).

REFERENCES

- 1 A.W.Leissa, "Vibration of plates", *Acoustical Society of America*, 1993.
- 2 A.W.Leissa, "The historical bases of the Rayleigh and Ritz", *J. Sound Vibration* 287, 961-978(2005).
- 3 M.Mukhopadhyay, "Free vibration of rectangular plates with edges having different degrees of rotational restraint", *J. Sound Vibration*, 67, 459-468(1979).
- 4 G.B.Warburton and S.L.Edney, "Vibrations of rectangular plates with elastically restrained edges", *J. Sound Vibration*, 95, 537-552(1984).
- 5 J.L.Horner and R.G.White, "Prediction of vibration power transmission through bends and joints in beam-like structures", *J. Sound Vibration*, 147, 87-103(1991).
- 6 D.J.Gorman, "Free in-plane vibration analysis of rectangular plates by the method of superposition", *J. Sound Vibration*, 272,831-851(2004).
- 7 W.L.Li, "Free vibration of beams with general boundary conditions", *J. Sound Vibration*, 237,709-725(2000).
- 8 J.C.Wohlever and R.J.Bernhard,"Mechanical energy flow models of rods and beams", *J. Sound Vibration*, 153, 1-19(1992).
- 9 N.H.Farag and J.Pan, "Dynamic response and power flow in two-dimensional coupled beam structures under in-plane loading", *J. Acoust. Soc. Am.* 99(1996), 2930-2937.
- 10 N.H.Farag and J.Pan, "On the free and forced vibration of single and coupled rectangular plates", *J. Acoust. Soc. Am.* 104, 204-216(1998).
- 11 J.M.Cuschieri,"Structural Power Flow Analysis Using a Mobility Approach of an L-shaped Plate", *J. Acoust. Soc. Am.* 871159-1165(1990).
- 12 J.M.Cuschieri and M.D.McCollum, "In-plane and out-of-plane waves' power transmission through an L-plate junction using the mobility power flow approach", *J. Acoust. Soc. Am.* 100, 857-870(1996).

- 13 Nicole J.Kessissoglou, "Power transmission in L-shaped plates including flexural and in-plane vibration", *J. Acoust. Soc. Am.* 115, 1157-1169(2004).
- 14 A.N.Bercin and R.S.Langley, "Application of the dynamic stiffness technique to the in-plane vibration of plate structures", *Computers and Structures* 59, 869-875(1996).
- 15 B.R.Mace and P.J.Shorter, "Energy flow models from finite element analysis", *J.Sound Vibration* 233,369-389(2000).
- 16 Z.H.Wang, J.T. Xing and W.G.Price, "Power flow analysis of rod/beam systems using a substructure method", *J. Sound Vibration*, 249, 3-22(2002).
- 17 Z.H.Wang, J.T. Xing and W.G.Price, "an investigation of power flow characteristics of L-shaped plates adopting a substructure approach", *J. Sound Vibration*, 250, 627-648(2002).
- 18 D.Zhou, "Natural frequencies of rectangular plates using a set of static beam functions in the Rayleigh-Ritz method", *J. Sound Vibration* 189, 81-88(1996).
- 19 D.Zhou, "Natural frequencies of elastically restrained rectangular plates using a set of static beam functions in the Rayleigh-Ritz method", *Computers and Structures*, 57,731-735(1995).
- 20 W.L.Li,"Vibration analysis of rectangular plates with general elastic boundary supports", *J. Sound Vibration*, 273, 619-635(2004).
- 21 W.L.Li, Xefeng Zhang, Jingtao Du, Zhigang Liu, "An exact series solution for the transverse vibration of rectangular plates with general elastic boundary supports", *J. Sound Vibration*, 321, 254-269 (2009).
- 22 Jingtao Du, W.L.Li, Guoyong Jin, TiejunYang, Zhigang Liu, "An analytical method for the in-plane vibration analysis of rectangular plates with elastically restrained edges", *J. Sound Vibration* 306,908-927(2007).
- 23 J.T.Du, "Study on modelling methods for structural vibration, enclosed sound space and their coupling system subject to general boundary conditions", PhD thesis (in Chinese), Harbin Engineering University,2009.